

DIGITAL ACCELERATION CONTROL METHOD FOR PATH TRACKING CONTROL OF AN AUTONOMOUS MOBILE ROBOT

YINA WANG, SHUOYU WANG, RENPENG TAN AND YINLAI JIANG

School of Systems Engineering
Kochi University of Technology
185 Miyanokuchi, Tosayamada, Kami, Kochi 782-8502, Japan
{ 156013z; 138003t }@gs.kochi-tech.ac.jp; { wang.shuoyu; jiang.yinlai }@kochi-tech.ac.jp

Received May 2011; accepted August 2011

ABSTRACT. *Autonomous mobile robots are widely used in industry, ports, and agriculture because they have the necessary loading capability. So far, the path-tracking accuracy of these robots is low due to nonlinear friction in the wheels, center-of-gravity (COG) shifts and load changes caused by users. To address these issues, a dynamics model is derived that considers nonlinear friction, COG shifts, and load changes. Furthermore, a digital acceleration control algorithm is proposed to compensate for nonlinear friction. Finally, simulations are executed using the proposed method. The results demonstrate the feasibility and effectiveness of the proposed digital acceleration control method.*

Keywords: Autonomous mobile robot, Nonlinear friction, Digital acceleration control, Path-tracking

1. Introduction. Autonomous mobile robots which are widely used in industry, ports and agriculture have been the focus of much interest. Many applications require autonomous robots having good path-tracking performance.

When autonomous mobile robots are used in factory automation and outdoor environments to improve the efficiency of cargo transport, it is essential for them to transport the cargo at a high speed and to carry as much cargo as possible. However, because of the nonlinear friction at high speed and the center-of-gravity (COG) shifts and load changes caused by large loads, the accuracy of the path-tracking decreases and the autonomous mobile robot sometimes strays from the predefined path, which clearly increases the danger of hitting obstacles. Therefore, the path-tracking control problem is the most basic research topic for autonomous mobile robots. If the problem of nonlinear friction, COG shifts and load changes could be solved, the motion performance of the autonomous mobile robot would be further improved.

One of the authors participated in the research of motion control for mobile robots and proposed a digital motion control method for these robots [1]. This control method was based on two idealized conditions: the COG is the same as the geometric center and the friction is assumed to be linear. Researchers in [2] focused on the motion process of mechanical systems and proposed a motion control method to deal with the nonlinear friction of a robot manipulator with many degrees of freedom. The effectiveness of this method was demonstrated by experiment [3]. This method is now widely known as the digital acceleration control method [4]. Based on these previous studies, this paper derived a model for the autonomous mobile robot by considering the nonlinear friction, COG shifts and load changes. A digital acceleration controller was proposed to deal with the problem of nonlinear friction, COG shifts and load changes. Finally, the proposed digital acceleration control method is verified feasible and effective by simulations.

2. Structure and Modeling of the Autonomous Mobile Robot. The autonomous mobile robot used in this paper has two driving wheels and two free casters as shown in Figure 1(a). To develop the control law for the autonomous mobile robot, the kinematic and dynamic equations are derived based on the coordinate settings and structural model shown in Figure 1(b).

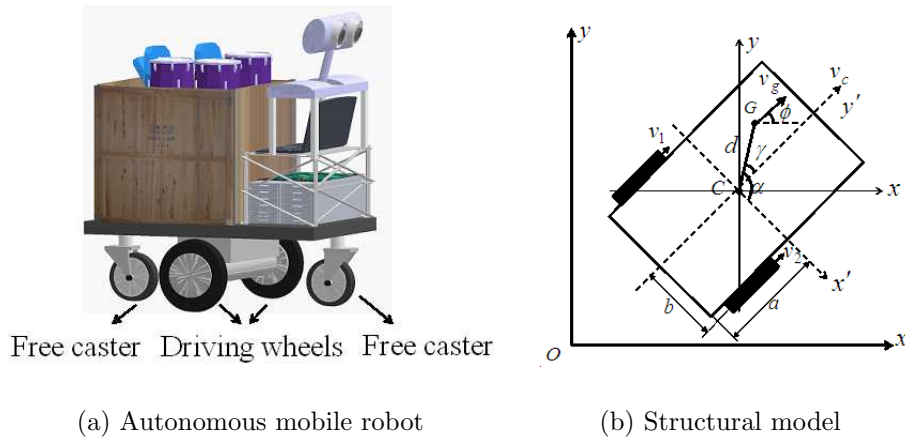


FIGURE 1. Autonomous mobile robot and its structural model

The parameters and coordinate system are as follows:

$\Sigma(x, y, O)$: absolute coordinate system; $\Sigma(x', y', C)$: translation coordinate system determined by the movement direction of the autonomous mobile robot; $G(x_g, y_g)$: position of the COG; $C(x_c, y_c)$: position of the geometrical center; v_g velocity at point G ; ϕ : angle between the direction of v_g and the x -axis; v_1, v_2 : velocities of the two driving wheels; α : angle between Cx' and CG ; γ : angle between CG and the Cy' ; $2b$: distance between the two driving wheels; $2a$: length of the autonomous mobile robot; d : distance between the COG and the geometrical center.

Using the coordinate system shown in Figure 1(b), by considering COG shifts, the kinematic equations are given as follows:

$$\begin{bmatrix} v_g \\ \dot{\phi} \end{bmatrix} = \begin{bmatrix} \frac{r(b + d \cos \alpha)}{2b} & \frac{r(b - d \cos \alpha)}{2b} \\ \frac{r}{2b} & -\frac{r}{2b} \end{bmatrix} \begin{bmatrix} \dot{\theta}_1 \\ \dot{\theta}_2 \end{bmatrix} \quad (1)$$

where r is the radius of driving wheels, $\dot{\phi}$ is the turning speed of the robot, and $\dot{\theta}_1$ and $\dot{\theta}_2$ are the speeds of two driving wheels.

According to the Lagrange formulation, the dynamic equations considering the COG shift and nonlinear friction are given as follows:

$$\begin{cases} \tau_1 = m_{11}\ddot{\theta}_1 + m_{12}\ddot{\theta}_2 + T_1(\theta_1, \dot{\theta}_1) \\ \tau_2 = m_{21}\ddot{\theta}_1 + m_{22}\ddot{\theta}_2 + T_2(\theta_2, \dot{\theta}_2) \end{cases} \quad (2)$$

where

$$\begin{aligned} m_{11} &= \frac{r^2(M + m)}{4b^2}(b + d \cos \alpha)^2 + \frac{r^2[I + d^2(M + m)]}{4b^2} + (J_\omega + k^2 J_0) \\ m_{12} &= \frac{r^2(M + m)}{4b^2}(b + d \cos \alpha)(b - d \cos \alpha) - \frac{r^2[I + d^2(M + m)]}{4b^2}, \quad m_{21} = m_{12} \\ m_{22} &= \frac{r^2(M + m)}{4b^2}(b - d \cos \alpha)^2 + \frac{r^2[I + d^2(M + m)]}{4b^2} + (J_\omega + k^2 J_0) \end{aligned}$$

where M is the mass of the autonomous mobile robot; m is the equivalent mass that loads imposes on the robot; I is the moment of inertia of the autonomous mobile robot;

J_ω is the moment of inertia of the driving wheels, J_0 is the moment of inertia of the DC motors, and k is the gear ratio.

τ_1 and τ_2 denote the driving torque acting upon the two driving wheels, $\ddot{\theta}_1$ and $\ddot{\theta}_2$ denote the acceleration of the two wheels, and T_1 and T_2 denote the nonlinear friction torque given as follows:

$$T_i = c_i \dot{\theta}_i + \begin{cases} \tau_i & \dot{\theta}_i = 0 \text{ and } \tau_i < T_{\max i} \\ T_{\max i} & \dot{\theta}_i = 0 \text{ and } \tau_i \geq T_{\max i} \\ T_{\min i} + (T_{\max i} - T_{\min i})e^{-a_i \dot{\theta}_i} & \dot{\theta}_i > 0 \\ -T_{\min i} + (T_{\min i} - T_{\max i})e^{a_i \dot{\theta}_i} & \dot{\theta}_i < 0 \end{cases}, \quad (i = 1, 2) \quad (3)$$

The nonlinear friction contains the viscous friction which mainly results from the contact between the wheels and the axle, and the coulomb friction which mainly results from the contact between ground and the wheels. c_i is the viscous friction coefficient; $T_{\max i}$ is the maximum static friction torque, and $T_{\min i}$ is the minimum sliding friction torque.

3. Controller Design. In this section, we develop an acceleration control method for the autonomous mobile robot [4]. Firstly, the control torque is kept constant between every time period of length T , let kT^+ is the instant after the change of the control torque at time kT . For a constant sampling period T , at times $t = kT^+$ and $t = kT$, we can obtain (4) as

$$\begin{aligned} \tau[kT] &= \mathbf{M}\ddot{\boldsymbol{\theta}}(kT) + \mathbf{T}[\boldsymbol{\theta}(kT), \dot{\boldsymbol{\theta}}(kT)] \\ \tau[kT^+] &= \mathbf{M}\ddot{\boldsymbol{\theta}}(kT^+) + \mathbf{T}[\boldsymbol{\theta}(kT^+), \dot{\boldsymbol{\theta}}(kT^+)] \end{aligned} \quad (4)$$

where $\tau[(k - 1)T^+] = \tau[kT]$ is the control torque during $[(k - 1)T^+, kT]$, and $\tau[kT^+] = \tau[(k + 1)T]$ is the control torque during $[kT^+, (k + 1)T]$. At times $t = kT^+$ and $t = kT$ the velocity, position and nonlinear friction are constant, but the acceleration is changed. Considering the nonlinear system (2) with control (5).

$$\begin{aligned} \begin{bmatrix} \tau_1(kT^+) \\ \tau_2(kT^+) \end{bmatrix} &= \begin{bmatrix} \tau_1[(k - 1)T^+] \\ \tau_2[(k - 1)T^+] \end{bmatrix} + \mathbf{M} \left\{ \begin{bmatrix} \ddot{\theta}_1^*(kT^+) - \ddot{\theta}_1(kT) \\ \ddot{\theta}_2^*(kT^+) - \ddot{\theta}_2(kT) \end{bmatrix} \right. \\ &\quad \left. + K_D \begin{bmatrix} \dot{\theta}_1^*(kT) - \dot{\theta}_1(kT) \\ \dot{\theta}_2^*(kT) - \dot{\theta}_2(kT) \end{bmatrix} + K_P \begin{bmatrix} \theta_1^*(kT) - \theta_1(kT) \\ \theta_2^*(kT) - \theta_2(kT) \end{bmatrix} \right\} \end{aligned} \quad (5)$$

where $K_D = \text{diag}(k_{d1}, k_{d2})$ and $K_P = \text{diag}(k_{p1}, k_{p2})$ are the speed deviation coefficient and position deviation coefficient, respectively. Here, K_D and K_P are always 2×2 diagonal positive-definite matrices.

Let $\mathbf{e}(kT^+) = \boldsymbol{\theta}^*(kT^+) - \boldsymbol{\theta}(kT^+)$ be the tracking error of the target trajectory, substituting into (5) using (4) yields

$$\ddot{\mathbf{e}}(kT^+) + K_D \dot{\mathbf{e}}(kT^+) + K_P \mathbf{e}(kT^+) = 0 \quad (6)$$

In the short time interval of $[kT^+, (k + 1)T]$, Equation (7) holds.

$$\begin{aligned} \dot{\mathbf{e}}[(k + 1)T^+] &= \dot{\mathbf{e}}(kT^+) + \ddot{\mathbf{e}}(kT^+)T \\ \mathbf{e}[(k + 1)T^+] &= \mathbf{e}(kT^+) + \dot{\mathbf{e}}(kT^+)T + \ddot{\mathbf{e}}(kT^+)T^2/2 \end{aligned} \quad (7)$$

Using (6) and (7) we can obtain

$$\begin{bmatrix} \mathbf{e}[(k + 1)T^+] \\ \dot{\mathbf{e}}[(k + 1)T^+] \end{bmatrix} = \begin{bmatrix} I - K_P T^2/2 & (I - K_D T/2)T \\ -K_P T & I - K_D T \end{bmatrix} \begin{bmatrix} \mathbf{e}[kT^+] \\ \dot{\mathbf{e}}[kT^+] \end{bmatrix} = A \begin{bmatrix} \mathbf{e}[kT^+] \\ \dot{\mathbf{e}}[kT^+] \end{bmatrix} \quad (8)$$

Here, K_D, K_P are designed to ensure that all eigenvalues of A are within the unit circle. Then, $\lim_{k \rightarrow \infty} \mathbf{e}(kT) = \lim_{k \rightarrow \infty} [\boldsymbol{\theta}^*(kT) - \boldsymbol{\theta}(kT)] = 0$ is obtained. Therefore, the system is stable. Furthermore, $\lim_{k \rightarrow \infty} x_c = x_c^*, \lim_{k \rightarrow \infty} y_c = y_c^*, \lim_{k \rightarrow \infty} \phi = \phi^*$, the path-tracking is accomplished. Figure 2 shows the block diagram of the control system presented in (5).

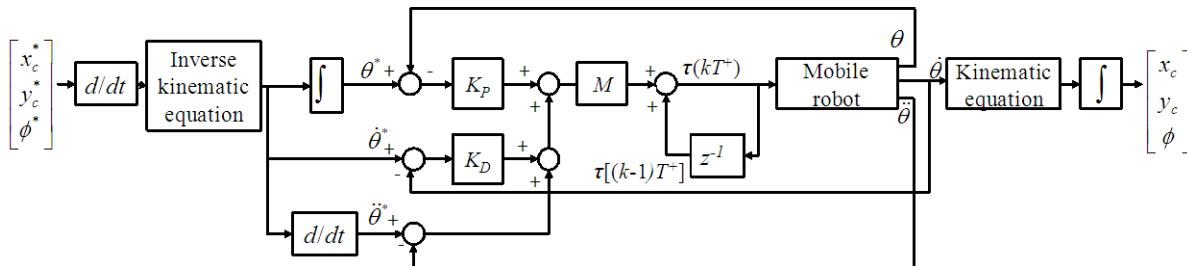


FIGURE 2. Block diagram of the digital acceleration control system

4. **Simulation.** In this section, the effectiveness of digital acceleration controller to deal with nonlinear friction is verified by circular path tracking simulations. The physical parameters of the autonomous mobile robot used in the simulations are given below. $M = 46.5$ kg, $m = 60$ kg, $b = 0.27$ m, $d = 0.2$ m, $r = 0.122$ m, $I = 1.3133$ kg·m², $\gamma = \pi/6$ rad, $\alpha = 2\pi/3$ rad, $c_1 = c_2 = 02$ kg·m/s, $a_1 = a_2 = 500$ m²/s, $T_{\max 1,2} = 60$ N·m, $T_{\min 1,2} = 6$ N·m, $J_0 = 0.0125$ kg·m², $J_w = 0.0144$ kg·m² and $k = 3$.

The trajectory is described by

$$\begin{aligned} x_c^*(t) &= x_0 + r \cos \sigma(t) \\ y_c^*(t) &= y_0 + r \sin \sigma(t), \quad \sigma(t) = \begin{cases} \frac{4\pi}{t_0^2} t^2 & 0 \leq t \leq \frac{t_0}{2} \\ 2\pi - \frac{4\pi}{t_0^2} (t - t_0)^2 & \frac{t_0}{2} < t \leq t_0 \end{cases} \\ \phi^*(t) &= \frac{\pi}{2} + \sigma(t) \end{aligned} \tag{9}$$

$(x_0, y_0) = (5 \text{ m}, 5 \text{ m})$ specifies the center of the circle, $r = 4 \text{ m}$ is the radius, and $t_0 = 150$ s. The initial position $x_c(0) = 8 \text{ m}$, $y_c(0) = 4 \text{ m}$ and the initial angle $\phi(0) = 0$ rad. The parameters of the digital acceleration controller are adjusted in the simulation for the condition of no nonlinear friction ($T_1 = T_2 = 0$).

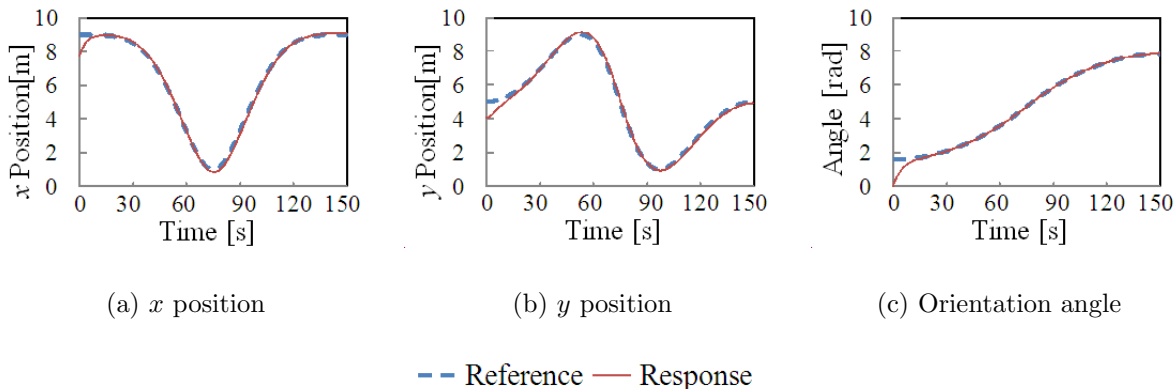


FIGURE 3. Simulation results of digital acceleration controller without nonlinear friction

Figure 3 and Figure 5(a) show the tracking performance of the autonomous mobile robot using the proposed digital acceleration algorithm when nonlinear friction is not considered,. Compared with Figure 3 and Figure 5(a), Figure 4 and Figure 5(b) show the tracking performance of the autonomous mobile robot when nonlinear friction is considered, with no changes to the other parameters. In Figures 3(a)-3(c) and Figures 4(a)-4(c), the horizontal axes is the simulation time (the maximum is 150 s), and the vertical axes are x position, y position, and time-variant orientation angle, respectively. Figure 5(a) and Figure 5(b) show the tracking and gradient of the autonomous mobile robot. In Figure 4 and Figure 5(b), the response curve is similar to that in Figure 3 and Figure 5(a), which indicates that the proposed digital acceleration algorithm can successfully track the

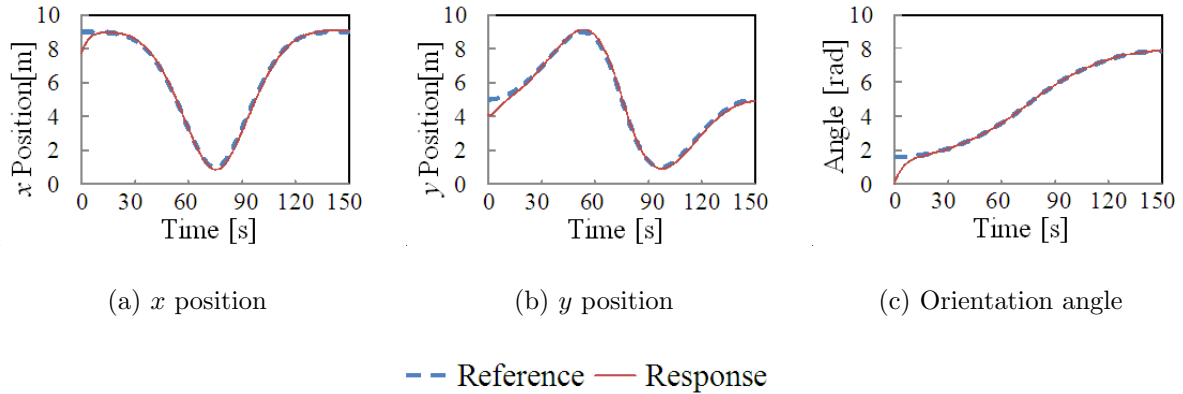


FIGURE 4. Simulation results of digital acceleration controller with nonlinear friction

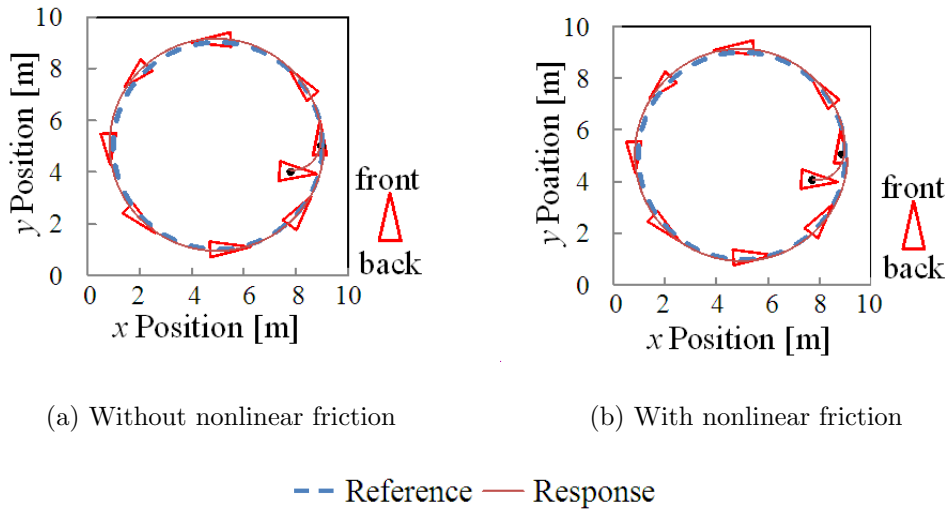


FIGURE 5. Tracking and gradient results with proposed control method

circular path rapidly and accurately even if nonlinear friction exists in the system. Thus, the digital acceleration controller effectively deals with the effect of nonlinear friction in the system.

Although only a circular path is considered in the simulation, the performance with respect to x position, y position, and orientation angle was all tested. The simulation results show that the proposed digital acceleration control method is feasible and effective to deal with the nonlinear friction. Because the control torque of the previous sampling period includes the effect of nonlinear friction, the current control torque could compensate for nonlinear friction based on the nonlinear friction of the previous sampling period. Therefore, the proposed digital acceleration controller can allow the controlled system to compensate for a greater level of nonlinear friction, which was verified by the simulations.

5. Conclusions. In this paper, to improve the path-tracking performance of an autonomous mobile robot, nonlinear friction existing in wheels, COG shifts and load changes are considered. A digital acceleration control algorithm is proposed for motion control of the mobile robot. The simulation results suggest that the proposed control method is feasible and effective. Therefore, the proposed control method is applicable for reducing path-tracking errors, showing its advantages in use.

Furthermore, not only the control method but also the trajectory planning method will be developed to improve the path tracking performance.

REFERENCES

- [1] Y. Hashimoto, S. Wang, T. Tsuchiya and T. Matsuda, Path-tracking of wheeled mobile robot using preview and predictive control, *Journal of the Robotics Society of Japan*, vol.12, no.4, pp.630-637, 1994 (in Japanese).
- [2] S. Wang, T. Tsuchiya and Y. Hashimoto, The digital acceleration control method of robot manipulator, *Proc. of the 1st Symposium on Robot Robotics Society of Japan*, vol.1, pp.7-12, 1991 (in Japanese).
- [3] S. Wang, T. Tsuchiya and Y. Hashimoto, Path tracking control of robot manipulators utilizing future information of desired trajectory, *Transactions of the Japan Society of Mechanical Engineers*, vol.59, no.564C, pp.2512-2518, 1993 (in Japanese).
- [4] T. Tsuchiya and K. Fukaya, *Introduction of Mechatronics*, Morikita Publishing Co., Tokyo, 2004.